

Published in final edited form as:

*J Urol.* 2011 September ; 186(3): 1107–1113. doi:10.1016/j.juro.2011.04.109.

## Ultrastructural Investigation of Crystal deposits in Npt2a knockout mice: Are they similar to Human Randall's plaques?

Saeed R. Khan and

Department of Pathology, Immunology and Laboratory Medicine, And Center for the Study of Lithiasis

Benjamin K. Canales

Department of Urology, University of Florida, Gainesville, Florida 32610

### Abstract

**Purpose**—Idiopathic calcium oxalate (CaOx) stones are suggested to develop attached to renal interstitial calcium phosphate (CaP) deposits, the Randall's plaques (RP), Sodium phosphate co-transporter (Npt2a) null mice are hypercalciuric, hyperphosphaturic, and produce tubular and interstitial CaP deposits. To determine if this mouse is suitable for RP investigations, we chronologically studied their location, structure, and composition.

**Materials and Methods**—Kidneys of Npt2a null mice of two days to a year old were examined by light, scanning (SEM) and transmission electron microscopy (TEM). Electron diffraction and energy dispersive x-ray microanalyses were performed to determine the mineral composition.

**Results**—Poorly crystalline biological apatite deposits were seen in lumens of collecting ducts. Deposits consisted of aggregates of approx 5 $\mu$ m diameter microspheres of concentrically organized needle or plate-like matrix rich crystals. Epithelium/ crystal interfaces were filled with membrane bound vesicles. Some tubules were completely occluded by crystals, occasionally lost their epithelium and crystals moved into the interstitium.

**Conclusions**—CaP crystals formed in tubular lumen and organized as microspheres. The aggregation of CaP crystals produced nuclei, which grew by the addition of crystals on periphery, eventually becoming large enough to occlude tubular lumen and obliterate tubular epithelium, leading to the relocation of microliths into interstitium. The pathogenesis of interstitial deposits of the Npt2a null mice appears different from that proposed for RP's. Since Npt2a null mice purge their renal crystal deposits, these mice may serve as a model to investigate elimination of crystal deposits seen in children and adults with nephrocalcinosis

### Keywords

Randall's Plaque; Calcium Phosphate; Nephrocalcinosis; Sodium phosphate co-transporter; Nephrolithiasis; Stone Formation

---

© 2011 American Urological Association. Published by Elsevier Inc. All rights reserved.

**Publisher's Disclaimer:** This is a PDF file of an unedited manuscript that has been accepted for publication. As a service to our customers we are providing this early version of the manuscript. The manuscript will undergo copyediting, typesetting, and review of the resulting proof before it is published in its final citable form. Please note that during the production process errors may be discovered which could affect the content, and all legal disclaimers that apply to the journal pertain.

## Introduction

Calcium oxalate nephrolithiasis is a common urological disorder afflicting 10-15% of the population in Europe and America.<sup>1</sup> Hypercalciuria and higher supersaturation with respect to calcium oxalate (CaOx) and calcium phosphate (CaP) are shared features of these stone formers.<sup>2</sup> Renal phosphate leak, and associated phosphaturia are significant underlying abnormalities of many recurrent stone formers.<sup>3</sup> The idiopathic CaOx stones generally include some CaP,<sup>4</sup> and develop attached to Randall's<sup>5</sup> plaques which are renal papillary sub-epithelial interstitial deposits of poorly crystalline biological CaP. Currently, the mechanism of formation and development of the plaque is unclear. A number of rat and mouse models of hypercalciuria have been developed. So far, hypercalciuria has led only to intratubular deposition of CaP in rats.<sup>6-8</sup> Mice deficient in Tamm-Horsfall protein demonstrate progressive calcification in renal papillae located more frequently in the renal interstitium than in the renal tubules.<sup>9</sup> Two genetically modified mice models of hypercalciuria, the type IIa sodium dependent phosphate co transporter (Npt2a) null and sodium/hydrogen exchanger regulatory factor -1 (NHERF) null, however, produce CaP crystals, some of which appear to be located in the renal interstitium.<sup>10-12</sup> Randall's plaques comprise of poorly crystalline biological CaP and are suggested to start in the basement membrane of the loops of Henle.<sup>13, 14</sup> To determine the location and mineral composition of the CaP deposits in hypercalciuric mice we carried out electron microscopic studies of the kidneys of Npt2a knockout mice. Inactivation of Npt2a gene results in increased urinary excretion of phosphate and calcium and CaP deposition in the kidneys.

## Materials and Methods

Mice with disrupted Npt2a co-transporter gene (Npt2a<sup>-/-</sup>) were created by targeted mutagenesis.<sup>15</sup> We received as a gift, male and female (Npt2a<sup>-/-</sup>, Npt2a<sup>+/-</sup>) mice from Dr. Tenenhouse and established a colony at the University of Florida. The genotype was determined by polymerase chain reaction amplification of genomic DNA extracted from mice tails using *Taq* polymerase. Npt2a<sup>-/-</sup> are viable and fertile with normal gross appearance. Npt2a<sup>-/-</sup> (KO) mice develop intratubular deposits of apatitic CaP.<sup>11</sup> Deposits are present in newborn, weanling as well as adult mice. To determine the effect of age on urinary chemistry, urine was collected from male and female mice ranging in age from 3 to 11 months. The urine was analyzed for calcium, phosphorus, creatinine, magnesium, sodium and potassium.

The kidneys were removed, decapsulated, and cut in half. One half was placed in buffered formalin and processed for light microscopic (LM) investigation. The other half was placed in a glutaraldehyde-formaldehyde mixture for scanning (SEM) and transmission (TEM) electron microscopic studies. Paraffin embedded sections were stained with hematoxylin and eosin (H&E) as well as von Kossa.<sup>10</sup> Selected sections were also stained with PAS and for osteopontin. The kidneys of 5 days old pups were examined by SEM and TEM following standard techniques. Some samples were demineralized before processing for TEM. 5-10  $\mu$ m paraffin-sections were mounted on cover slips, deparaffinized, dehydrated and dried in a vacuum cabinet. The cover slips were mounted on an aluminum stub, coated with carbon, platinum or gold palladium and examined using a SEM equipped with energy dispersive x-ray microanalysis.

## Results

Table 1 shows urinary chemistry of male and female Npt2a null mice of different ages. As we reported earlier<sup>10</sup>, there were no noticeable differences between the urine from the male and female mice. In addition, age of the mice, from 3 to 11 months, did not appear to have

an effect on the various urinary factors which were analyzed. We could not obtain sufficient urine for analyses from the weanling mice.

Light microscopic examination of the von-Kossa stained kidneys from 2 and 5 days old mice showed abundant CaP deposition (Figure 1). The outer medulla contained the most crystal deposits which were typically located in the renal tubular lumens with few in the renal interstitium as well. Crystal matrix and epithelial cells of adjacent renal tubules stained positive for osteopontin. It was observed that as mice matured, a number of crystal deposits disappeared, resulting in the year old mice exhibiting very few crystals<sup>10</sup>.

TEM examination showed that crystal deposits, where tubular ultra structure could be determined, were located in lumens of the collecting ducts. They were, identified by their cuboidal appearance, relatively smooth luminal plasma membrane, a single cilium and few cytoplasmic organelles (Figure 2). The deposits were comprised of approximately 100-110 nm long thin plate-like crystals which appeared variously distributed and organized, at times as starbursts and others as microspheres or spherulites. The spherulites often appeared lying loosely in the tubular lumens surrounded by cellular degradation products. Individual spherulites were approximately 5 $\mu$ m across, laminated and consisted of concentrically arranged thin 100-110 nm long plate like crystals.

Some deposits completely filled the tubular lumens (Figure 3). In some instances these microliths grew so big, as large as 170  $\mu$ m across, that they obliterated the tubular epithelium. Occasionally even the basement membrane disappeared and the entire microlith was seen located in the interstitium surrounded by blood vessels, peritubular cells, collagen fibers, membrane bound vesicles etc (Figure 4).

Examination of demineralized deposits demonstrated the ubiquitous nature of matrix and its intimate association with the mineral which resulted in the formation of poorly crystalline biological apatite. Microliths contained a nucleus of aggregated spherulites and cell debris surrounded by concentrically arranged layers of crystals similar to growth rings of an old tree. Larger microliths showed more layers (Figure 3B). A number of secondary nucleation sites appeared to develop on surface of the growing microliths and developed their own semicircular laminations. Selected area electron diffraction identified poorly crystalline biological apatite.

Often, the crystals came in close contact with the apical plasma membrane of the epithelial cells (Figure 4). Generally the interface showed membrane and membrane bound vesicles intimately associated with the surface crystals. At times, however, the contact was so close that it was difficult to separate the crystals from the plasma membrane. Cells in contact with the luminal crystals generally appeared normal with normal looking mitochondria, active golgi apparatus, and endoplasmic reticulum. However, signs of tubular and interstitial cell degradation were also evident. Tubular lumens were filled with cell debris. Proximal tubular epithelial cells contained a highly active endocytic system with large number of apical cytoplasmic vesicles.

SEM analyses of the crystal deposits showed a rough surface with plate-like projections. Examination of the fractured surface showed it to be unremarkable with few laminations. Energy dispersive analysis showed that calcium to phosphorus ratio was higher in the outer layers than the inner ones.

## Discussion

The Npt2a sodium-dependent co-transporters located on the apical membrane of the renal proximal tubular epithelial cells are essential for the maintenance of phosphate homeostasis.

Targeted deletion of *Npt2a* gene in mice resulted in increased urinary excretion of Pi, ~80% decrease in renal brush border membrane Na/Pi co-transport, and hypophosphatemia, which led to increased serum 1,25 (OH)<sub>2</sub>D levels, over expression of intestinal calcium channels, increased intestinal calcium hyperabsorption and development of hypercalcemia and hypercalciuria.<sup>16</sup> *Npt2a* has a PDZ binding domain enabling it to bind PDZ proteins including NHERF-1,<sup>12,17</sup> which is involved in regulating *Npt2a* transcription and protein processing. Genetic variants of human NPT2a have been reported but are not shown to be a cause of renal phosphate leak.<sup>18</sup> A mutation in NPT2c has however been identified as the cause of hypophosphatemic rickets with hypercalciuria.<sup>19</sup> A mutation in the NHERF-1 gene has been reported to produce phosphaturia.<sup>20</sup> Young male and female NHERF-1 null mice are hypophosphatemic, and excrete increased amounts of phosphate and calcium in their urine. However, urinary excretion of phosphate declines with age reaching normal levels by age of 30 weeks. Both *Npt2a* null as well as NHERF-1 null mice produce CaP crystal deposits. New born *Npt2a* null mice demonstrate a large number of CaP deposits in all zones of their kidneys. However, the number of CaP deposits declines with age and by 11 month only a few are seen, mostly observed in the renal papillae.<sup>10</sup> On the other hand NHERF-1 null have been shown to produce only a few deposits in renal papillae of 54 week old mice.<sup>12</sup> Younger NHERF-1 null mice have not been investigated for the deposition of CaP crystals and it is likely that like *Npt2a* null mice, they also demonstrate an age dependent crystal deposition.

The results of the present study demonstrate for the first time that most CaP crystals deposit in lumens of the collecting ducts attached to the epithelial apical plasma membranes and associated with nearby membrane bound vesicles or are free in the primary urine mixed with membranous cellular degradation products. Few interstitial deposits were seen. They were also associated with membrane bound vesicles. Primary urine is generally concentrated when it reaches the collecting ducts and in the presence of high calcium and phosphate as is the case in *Npt2a* null mice, would be supersaturated with respect to CaP. This should be sufficient to promote nucleation and growth of CaP crystals in the collecting ducts. However, the kidneys of new born mice are still growing and tissue is remodeling with necrosis and apoptosis and cells are being sloughed into the urine. The presence of membranes in the already supersaturated urine would further influence the nucleation process and may even assist in crystal aggregation.<sup>21</sup> A number of *in vitro* studies have shown that membranous cellular debris can promote nucleation of calcific crystals at a lower supersaturation.<sup>22</sup> Alternatively, intratubular deposits seen in *Npt2a* null mice may arise similar to those seen in the female weanling rats given AIN-76 diet. The rats became hypercalciuric and produced intratubular concretions of CaP. Calcification started in association with calcium rich vesicles budding from the brush border of the proximal tubular epithelium.<sup>8</sup>

The results also demonstrate that some luminal crystal deposits continued to grow and eventually filled the entire tubular lumen. Growth of such microliths appears to have occurred by addition of crystals on the surface.. Apparently the tubule-occluding well developed microliths caused degeneration of the renal epithelium. The loss of tubular epithelium led to relocation of the microlith from tubular lumen into the interstitium. Movement of crystals from tubular lumen into the renal interstitium has been previously reported.<sup>23, 24</sup> However, that movement was through regeneration of tubular epithelium and migration of cells over the retained crystals.

Randall suggested two pathways to the formation of kidneys stones.<sup>5</sup> In his pathway 1, stones formed attached to subepithelial precalculus lesions on the renal papillary surface. The lesion itself started as poorly crystalline carbonate apatite in the papillary interstitium. Pathway 2 involved crystal deposition in lumens of the ducts of Bellini as the result of high

supersaturation. Currently Randall's plaque generally refers to type 1 precalculus lesion and is suggested to start as laminated microspheres of poorly crystalline biological apatite in basement membrane of the loops of Henle.<sup>14</sup> These microspheres are suggested to migrate to the subepithelial space, coalesce with others and materialize as Randalls' plaque. Once exposed to the pelvic urine the plaque is overgrown by CaOx crystals and a stone is born.<sup>13</sup> Even though kidneys of most idiopathic stone formers have Randall's plaques, all of them do not have attached stones.

Morphology as well as morphogenesis of CaP deposits in the Npt2a null mice and Randall's plaques demonstrate similarities as well as dissimilarities. Both develop in kidneys of hypercalciuric individuals and start as matrix rich laminated microspheres of poorly crystalline biological apatite with an approximate diameter of 5 $\mu$ m. These microspheres then aggregate or coalesce and become a substrate for further crystal deposition. Final products, the Randall's plaques of human kidneys and interstitial CaP deposits of mice have similar appearance. These common features may be specific to crystallization in the kidneys or represent a general phenomenon in biological mineralization.<sup>25</sup> But sites of initiation are different. CaP deposits of Npt2a null mice are originally located in the tubular lumens while Randall's plaques are suggested to start in the basement membrane of the loops of Henle. But do these crystals actually start where they have been found at the time of investigation? In the case of Npt2a null mice kidneys have been examined in weanling, adult and old mice.<sup>10, 11</sup> Number of crystals decreased with age. The kidneys of newborn mice generally contained luminal crystals which disappeared as the mice aged<sup>10</sup>. The kidneys of older mice had interstitial crystals only. A range of crystal sizes from single microspheres to microliths were observed in the tubular lumens. A few luminal deposits were partially located in the interstitium while others were totally interstitial. Randall's plaques were obtained at the time of stone removal, long after stone formation. CaP crystals could have originated in the tubular lumens, and relocated to the interstitium as has been shown in the Npt2a null mice here and suggested by various, clinical, animal model and tissue culture studies.<sup>24, 26, 27</sup> That this may possibly be the case is also suggested by the reported lack of any obvious injury around the Randall's plaques of idiopathic stone formers<sup>13</sup> despite experimental data that all crystals are injurious to renal epithelial cells.<sup>28</sup> Interstitial CaP crystals of Randall's plaques are also shown to be positive for osteopontin, which is generally secreted into the lumen and could have become part of the crystal matrix before their relocation into the interstitium. The rationale given for crystal deposition in the basement membrane of the loops of Henle is that urine concentration is maximal in this segment because water is reabsorbed in the loops. As a result supersaturation for CaP is significantly high in the loops of Henle promoting apatite formation. This should actually lead to apatite formation in the lumen and not the interstitium.

Intratubular deposition of CaP is common in both children<sup>29</sup> and adults including many non-idiopathic stone formers<sup>30</sup>. Such deposits have deleterious effect on renal structure and function. Because of the Npt2a null mice ability to get rid of the deposits, these mice may be useful in investigating the mechanisms involved in elimination of the renal tubular crystalline deposits.

## Acknowledgments

Research supported by grant # RO1 DK078602 from NIDDK. We are thankful to Drs. JW Verlander, LB Gower and SJ Homeijer as well as Electron Microscopy Core for scanning and transmission electron microscopy of the specimens.

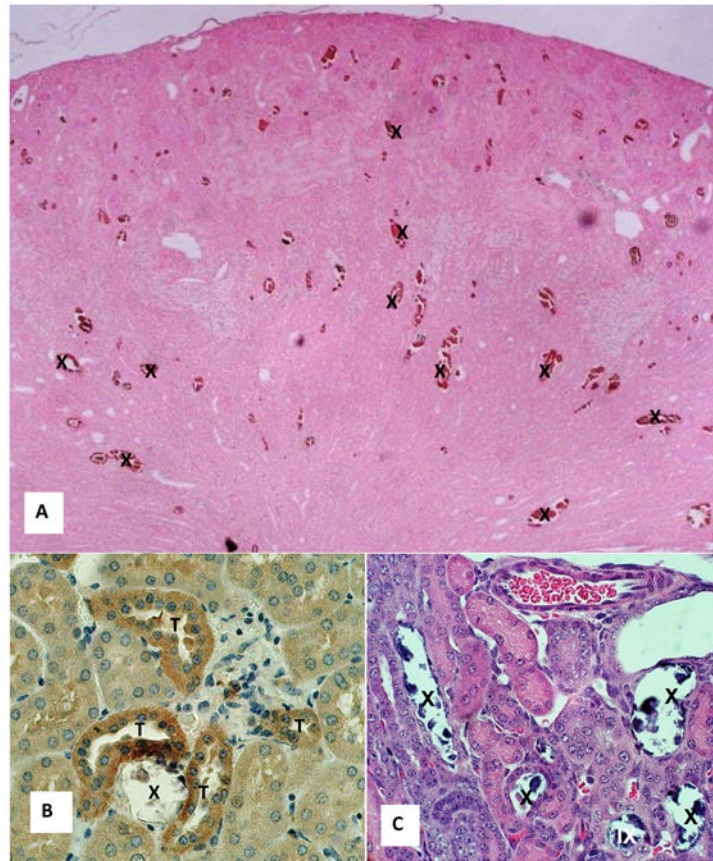
## References

1. Pearle MS, Calhoun EA, Curhan GC. Urologic diseases in America project: urolithiasis. *J Urol.* 2005; 173:848. [PubMed: 15711292]
2. Finlayson B. Physicochemical aspects of urolithiasis. *Kidney Int.* 1978; 13:344. [PubMed: 351263]
3. Prie D, Beck L, Silve C, et al. Hypophosphatemia and calcium nephrolithiasis. *Nephron Exp Nephrol.* 2004; 98:e50. [PubMed: 15499207]
4. Khan SR. Calcium phosphate/calcium oxalate crystal association in urinary stones: implications for heterogeneous nucleation of calcium oxalate. *J Urol.* 1997; 157:376. [PubMed: 8976301]
5. Randall A. The Origin and Growth of Renal Calculi. *Ann Surg.* 1937; 105:1009. [PubMed: 17856988]
6. Bushinsky DA, Parker WR, Asplin JR. Calcium phosphate supersaturation regulates stone formation in genetic hypercalciuric stone-forming rats. *Kidney Int.* 2000; 57:550. [PubMed: 10652032]
7. Khan SR, Glenton PA. Deposition of calcium phosphate and calcium oxalate crystals in the kidneys. *J Urol.* 1995; 153:811. [PubMed: 7861545]
8. Nguyen HT, Woodard JC. Intranephronic calculosis in rats: an ultrastructural study. *Am J Pathol.* 1980; 100:39. [PubMed: 7395968]
9. Liu Y, Mo L, Goldfarb DS, et al. Progressive renal papillary calcification and ureteral stone formation in mice deficient for Tamm-Horsfall protein. *Am J Physiol Renal Physiol.* 299:F469. [PubMed: 20591941]
10. Khan SR, Glenton PA. Calcium oxalate crystal deposition in kidneys of hypercalciuric mice with disrupted type IIa sodium-phosphate cotransporter. *Am J Physiol Renal Physiol.* 2008; 294:F1109. [PubMed: 18337544]
11. Chau H, El-Maadawy S, McKee MD, et al. Renal calcification in mice homozygous for the disrupted type IIa Na/Pi cotransporter gene *Npt2*. *J Bone Miner Res.* 2003; 18:644. [PubMed: 12674325]
12. Weinman EJ, Mohanlal V, Stoycheff N, et al. Longitudinal study of urinary excretion of phosphate, calcium, and uric acid in mutant *NHERF-1* null mice. *Am J Physiol Renal Physiol.* 2006; 290:F838. [PubMed: 16249272]
13. Coe FL, Evan AP, Worcester EM, et al. Three pathways for human kidney stone formation. *Urol Res.* 38:147. [PubMed: 20411383]
14. Evan AP, Lingeman JE, Coe FL, et al. Randall's plaque of patients with nephrolithiasis begins in basement membranes of thin loops of Henle. *J Clin Invest.* 2003; 111:607. [PubMed: 12618515]
15. Beck L, Karaplis AC, Amizuka N, et al. Targeted inactivation of *Npt2* in mice leads to severe renal phosphate wasting, hypercalciuria, and skeletal abnormalities. *Proc Natl Acad Sci U S A.* 1998; 95:5372. [PubMed: 9560283]
16. Tenenhouse HS. Phosphate transport: molecular basis, regulation and pathophysiology. *J Steroid Biochem Mol Biol.* 2007; 103:572. [PubMed: 17270430]
17. Shenolikar S, Weinman EJ. *NHERF*: targeting and trafficking membrane proteins. *Am J Physiol Renal Physiol.* 2001; 280:F389. [PubMed: 11181400]
18. Lapointe JY, Tessier J, Paquette Y, et al. *NPT2a* gene variation in calcium nephrolithiasis with renal phosphate leak. *Kidney Int.* 2006; 69:2261. [PubMed: 16688119]
19. Jaureguiberry G, Carpenter TO, Forman S, et al. A novel missense mutation in *SLC34A3* that causes hereditary hypophosphatemic rickets with hypercalciuria in humans identifies threonine 137 as an important determinant of sodium-phosphate cotransport in *NaPi-IIc*. *Am J Physiol Renal Physiol.* 2008; 295:F371. [PubMed: 18480181]
20. Karim Z, Gerard B, Bakouh N, et al. *NHERF1* mutations and responsiveness of renal parathyroid hormone. *N Engl J Med.* 2008; 359:1128. [PubMed: 18784102]
21. Khan SR, Glenton PA, Backov R, et al. Presence of lipids in urine, crystals and stones: implications for the formation of kidney stones. *Kidney Int.* 2002; 62:2062. [PubMed: 12427130]
22. Fasano JM, Khan SR. Intratubular crystallization of calcium oxalate in the presence of membrane vesicles: an in vitro study. *Kidney Int.* 2001; 59:169. [PubMed: 11135069]

23. Vervaeet BA, Verhulst A, D'Haese PC, et al. Nephrocalcinosis: new insights into mechanisms and consequences. *Nephrol Dial Transplant*. 2009; 24:2030. [PubMed: 19297353]
24. Khan SR. Calcium oxalate crystal interaction with renal tubular epithelium, mechanism of crystal adhesion and its impact on stone development. *Urol Res*. 1995; 23:71. [PubMed: 7676537]
25. Ryall RL. The future of stone research: rummagings in the attic, Randall's plaque, nanobacteria, and lessons from phylogeny. *Urol Res*. 2008; 36:77. [PubMed: 18286270]
26. Kumar V, Farrell G, Yu S, et al. Cell biology of pathologic renal calcification: contribution of crystal transcytosis, cell-mediated calcification, and nanoparticles. *J Investig Med*. 2006; 54:412.
27. Verhulst A, Asselman M, De Naeyer S, et al. Preconditioning of the distal tubular epithelium of the human kidney precedes nephrocalcinosis. *Kidney Int*. 2005; 68:1643. [PubMed: 16164641]
28. Khan SR. Renal tubular damage/dysfunction: key to the formation of kidney stones. *Urol Res*. 2006; 34:86. [PubMed: 16404622]
29. Ammenti A, Pelizzoni A, Cecconi M, et al. Nephrocalcinosis in children: a retrospective multi-centre study. *Acta Paediatr*. 2009; 98:1628. [PubMed: 19572991]
30. Coe FL, Evan AP, Lingeman JE, et al. Plaque and deposits in nine human stone diseases. *Urol Res*. 38:239. [PubMed: 20625890]

## Glossary

<b>CaOx</b>	calcium oxalate
<b>CaP</b>	calcium phosphate
<b>Npt2a</b>	Type IIa sodium dependent phosphate co transporter
<b>NHERF</b>	sodium/hydrogen exchanger regulatory factor
<b>LM</b>	light microscopic
<b>TEM</b>	transmission electron microscopic
<b>SEM</b>	scanning electron microscopic
<b>H &amp;E</b>	hematoxylin and eosin
<b>PAS</b>	Periodic acid-Schiff
<b>KO</b>	knock out



- 1.** Light microscopic analysis of Npt2a null mice kidneys. **A.** Section of a paraffin embedded kidney of 5 days old mice stained with von Kossa showing calcium phosphate deposits (X) in the cortex and outer medulla. Reduced from x4. **B.** Section of a kidney of 5 days old mice stained for osteopontin. Crystals (X) disappeared during processing. Crystal associated matrix as well as epithelial cells of the adjoining tubules (T) stained positive. Reduced from x40. **C.** Hematoxylin and eosin stained section of 2 days old mice showing tubules occluded with the crystals (X), many of which disappeared during processing. A couple of crystals deposits appear located in the renal interstitium (IX). Reduced from x40.



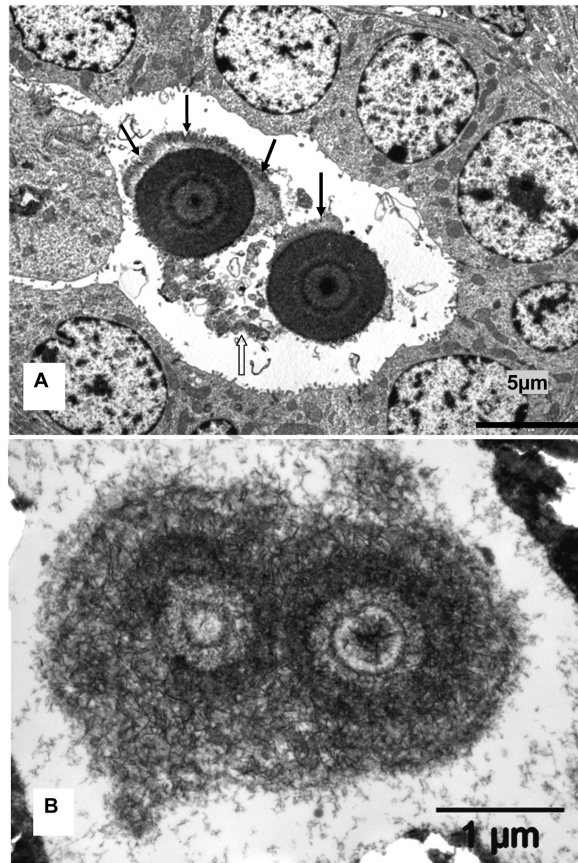


**Figure 2.** Transmission electron microscopic analysis of mice kidneys. **A.** Cross section of microsphereules of concentrically arranged thin plate-like crystals of CaP present in the lumen of a collecting duct. Approximately 5 μm across microsphereules are associated with cellular degradation products (clear arrow) and appear to be growing by addition of layer of crystals on the periphery (arrows). **B.** Higher magnification showing thin submicron size plate-like crystals starting in the center and organizing themselves into microsphereules.

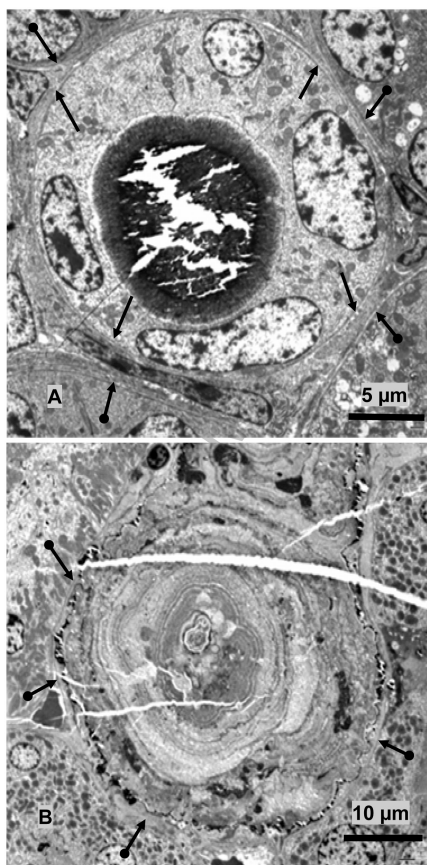


**Figure 3.**

TEM of Interface between crystal deposits and associated renal tissue. **A.** TEM of the cross section of a collecting duct. Large crystal deposit has filled the lumen lined with cuboidal cells with relatively smooth luminal plasma membrane and few cytoplasmic organelles. Both apical plasma membrane and the basement membrane (arrows) are intact. Basement membranes of the adjoining tubules are also visible (double headed arrows). **B.** TEM of the cross section of a large microlith completely obliterating the tubule which is surrounded by patent unobstructed tubules, with intact basement membrane (double headed arrows). Tissue was demineralized before processing. Crystal ghosts are arranged in concentric rings (arrow heads). Center of the microlith is filled with aggregating microspheres and cellular degradation products.

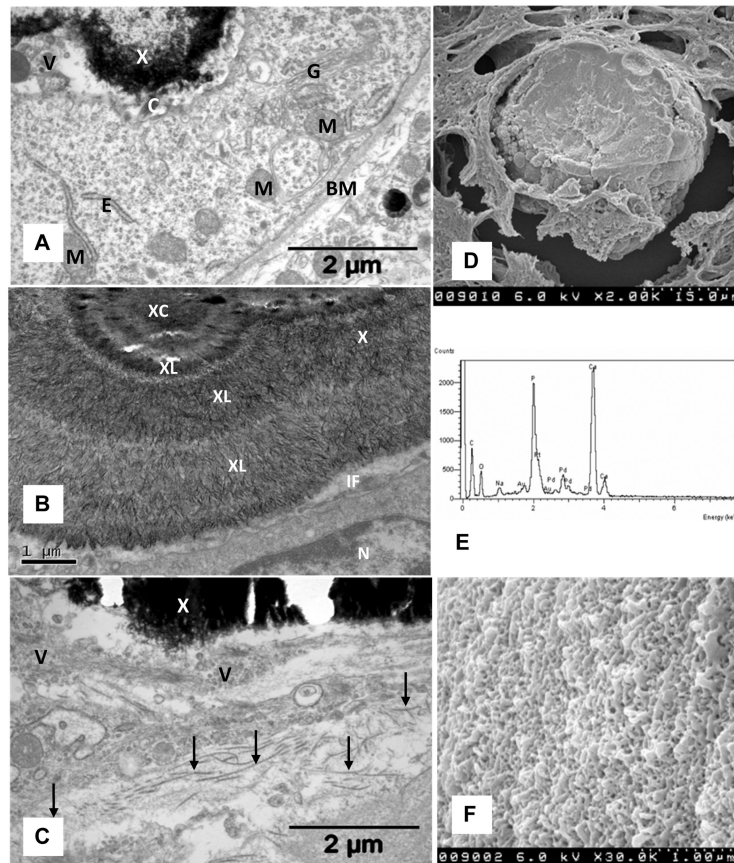


**Figure 4.**

Electron microscopical analyses of crystal deposits. **A.** Crystal deposit (X) adjacent to a tubular epithelial cell which shows active golgi apparatus (G), endoplasmic reticulum (E), mitochondria (M), cilium (C), basement membrane (BM). Interface between crystal and cell is filled with vesicles. **B.** High magnification showing nucleus (N) of an epithelial cell, a tight interface (IF) filled with small membrane bound vesicles. Crystal deposit shows a central area (XC) surrounded by concentric layers (XL) of radially organized thin plate-like crystals. **C.** Interstitially located crystal deposit (X) associated with membrane bound vesicles (V) of various sizes and collagen fibers (arrows). **D.** Scanning electron microscopy of the deposit completely filling the tubular lumen. **E.** Energy dispersive microanalysis of crystal deposit showing the presence of calcium (Ca) and phosphorus (P). **F.** High magnification of deposit surface showing variously arranged plate-like crystals (Compare with 2B, 4B).

Table 1

### Urinary Chemistry of male and female Npt2a null mice

Mice were housed in metabolic cages, three per cage. 24 hour urine was collected. Analysis was performed by the University of Florida Veterinary Diagnostic Laboratories.

	Male			Female		
	3 months	7 months	9 months	6 months	10 months	11 months
Calcium mg/dL	37.2	35.3	42.0	38.5	51.5	46.6
Phosphorus mg/dL	167.3	235.7	205.3	202.5	180.7	255.8
Creatinine mg/dL	36.7	65.6	58.8	51.9	53.2	66.6
Magnesium mg/dL	54.2	59.3	51.9	53.6	65.8	83.1
Sodium mmol/L	114.0	135.0	141.0	136.0	98.0	137.0
Potassium mmol/L	126.2	136.5	126.2	144.4	180.7	214.3